Available online at www.sciencedirect.com
SCIENCE DIRECT®
International Journal of Solids and Structures 42 (2005) 1957–1981
INTERNATIONAL JOURNAL OF SOLIDS and STRUCTURES
www.elsevier.com/locate/ijsolstr

Dispersion relations for cylindrical bending motions of polarized piezoceramic bimorph plates with two facing edges free

Jongwon Seok *

School of Mechanical Engineering, College of Engineering, Chung-Ang University, 221, Heukseok-Dong, Dongjak-Gu, Seoul 156-756, Korea

Received 18 April 2004; received in revised form 1 September 2004

Abstract

Dispersion relations of thin parallel bimorph plates with polarized piezoceramics are obtained by using Hamilton's principle. The coupled variational equations for piezoceramic bimorph plates are derived with the thin plate theory and the extension of electric potential in the thickness direction, which are valid for low frequency range. More specifically, coupled differential equations as well as dispersion relations subject to homogeneous natural-type boundary conditions on the two facing side-edges are derived for the cylindrical bending motions of both fully electroded and unelectroded bimorph plates of which surfaces are free from applied traction for both cases; the derivations are made through the expansions of mechanical displacements in the thickness co-ordinate with plane stress assumptions at major surfaces in the manner of Mindlin and of electric potential with vanishing second order components of electric potentials at major surfaces in the manner of Tiersten.

Relations between the deflection gradient of fully electroded bimorph plate and the induced electric current are obtained. The complexity due to the additional inclusion of differential equations for the electric potential components may be alleviated through the reductions of the coupled differential equations. As an illustrative example, dispersion relations for the aforementioned four cases of bimorph plates composed of PZT5 are obtained. The dispersion curves are depicted and compared each other, and some differences and similarities are discussed.

Keywords: Dispersion relations; Polarized piezoceramic bimorph plate; Reduction on differential equations; Fully electroded and unelectroded bimorph plates; Hamilton's principle

* Tel.: +82 2 820 5729; fax: +82 2 814 9476.
E-mail address: seokj@alum.rpi.edu

0020-7683/$ - see front matter © 2004 Elsevier Ltd. All rights reserved.
doi:10.1016/j.ijsolstr.2004.09.002

1. Introduction

Piezoelectric sensors and actuators are widely used to control shapes of mechanical structures (Anderson and Hagood, 1990; Rao and Sunar, 1994), to control vibrations (Chen et al., 1996) or to pick up vibratory signals for the measurement of physical quantities (Seok et al., in press). The main advantage of piezoelectric devices is that electric charge can be induced when the piezoelectric materials are mechanically deformed; on the contrary, mechanical stress and/or strain can be observed when an electric field is applied. The most useful forms of these devices generally take the form of laminated or bimorph in configuration.

A *laminated piezoelectric plate* is one of the most prominent applications of piezoelectric devices due to its simplicity, durability, and manufacturability. A *bimorph* is a bilaminar plate, which is a form of the laminated piezoelectric plate, consists of two piezoelectric plates attached each other. The bimorph plate, which is of interest in this work, has crystallographic axes of both layers in the same orientations and electrodes that are located on the middle surface of the two-layer plate and/or on its major surfaces. If an electric voltage were supplied to both layers, one layer would suffer elongation, while the other would suffer compression. This would result in cylindrical bending of the plate because both layers are attached and glued together.

Tiersten (1993) derived a system of approximate equations for the extensional and flexural motion of electroelastic plates subject to large electric field from the variational equation of electroelasticity. He used a usual series expansion for mechanical displacements but adopted a special form of series expansion of powers for electric potential in thickness co-ordinate to obtain approximate two-dimensional equations. He also derived two-dimensional equations for the flexural vibrations of symmetric composite plates with both unelectroded and electroded portions of piezoelectric actuators attached to the top and the bottom surfaces (Tiersten, 1995). In this work, he used the same series expansions for both mechanical displacements and electric potential as adopted in the previous paper to analyze cylindrical bending of a composite plate caused by the applied voltage. Ricketts (1993) performed a dynamic analysis for the transverse vibrations of composite piezoelectric plates. Although he obtained the eigensolutions of the plates using the Rayleigh method and the classical beam mode shapes, the approach was restricted to the assumed modal behaviors of the beam characteristic functions.

Cheng et al. (1999) developed a method to obtain solution for a laminated piezoelectric plate under uniform normal tractions and electric displacements using a transfer matrix method and asymptotic expansions in the framework of three-dimensional linear piezoelectricity theory. In this work, they investigated the ratio of in-plane and transverse electric field components and found that the in-plane electric field components can be significant under a certain conditions. At the same time, they also developed an asymptotic technique for anisotropic inhomogeneous and laminated piezoelectric plates with three-dimensional linear piezoelectricity theory (Cheng et al., 2000). Later, Lim and He (2001) analyzed the electromechanical responses of compositionally graded piezoelectric layers consisting of polycrystalline piezoelectric ceramics polarized along the thickness direction. They considered two cases for layers (i) with electrodes and (ii) without electrodes at major surfaces and obtained solutions for layers subjected to uniform mechanical loads in the sense of Saint Venant. However, only static problems were treated in their works.

In order to give more physical meaning to the shapes of stress functions, Lee et al. (1987) adopted a sinusoidal thickness expansion instead of the series expansion in powers of thickness co-ordinate in deriving the two-dimensional governing equations of piezoelectric crystal plates. Yong et al. (1993) developed a laminated plate theory for thickness-shear vibrations. To obtain the two-dimensional equations of motion for piezoelectric laminae in their work, the mechanical displacements and the electric potential were expanded in the series of trigonometric functions along the thickness co-ordinate, which is the identical to the method that Lee et al. (1987) used. Stewart and Yong (1994) later investigated acoustic wave propagation in multilayered anisotropic piezoelectric plates through the use of transfer matrix method. They obtained thickness

modes of and dispersion relations of straight crested waves propagating through two and three layered crystal plates with infinite planar dimensions. Rogacheva et al. (1998) analyzed the dynamic characteristics of a piezoelectric laminate cantilever beam using the similar series expansion to the previous literatures but with slightly different notations. They also performed an experiment for the verification of their results.

Keuning (1971) derived a two-dimensional approximate equation for a bimorph shell and solved the cylindrical bending problem by assuming the form of the solution based on the continuity conditions. One of the potential limitations of his work is that his model is confined to static cases. Nevertheless, he proved the validity of his assumptions by conducting an experiment with a good agreement to the theory developed in his paper. Another analysis for the piezoceramic bimorph plate was conducted by Steel et al. (1978). They investigated the features of electrical poling, hysteresis behavior, and transverse–longitudinal mechanical strain under the quasistatic assumptions. Fernandes and Pouget (2003) proposed an approach to piezoelectric bimorph plate using an expansion of the elastic displacement and electric potential through the thickness co-ordinate, in which they account for a shear correction and a layerwise modeling of the electric potential. In addition to these papers, Smits and Choi (1991) derived the constituent equations of piezoelectric heterogeneous bimorph by calculating the internal energy in thermodynamic equilibrium; Low and Guo (1995) modeled a three-layer piezoelectric bimorph beam in order to explain its hysteretic behavior; He et al. (2000) investigated three-dimensional electromechanical responses of an antiparallel piezoelectric bimorph, which is composed of two oppositely polarized piezoelectric plates having 6*mm* symmetry. They also used the transfer matrix method and asymptotic expansion, and showed that the only unknown functions in the expression of solution are the displacements on the mid-plane of the bimorph. Lim et al. (2001) later derived and solved a problem for three-dimensional parallel piezoelectric bimorph having 6*mm* symmetry using the state space method and the asymptotic expansion technique.

While numerous piezoelectric bimorph plate theories have been developed to obtain mechanical and electrical field quantities, most of these works are mainly for the static problems or for the dynamic problems with infinite planar dimensions or Levy-type boundary conditions, and the authors could not find any work on the dispersion relations of flexural waves propagating through an infinitely long polarized piezoceramic bimorph plate with two traction-free opposite edges in the open literature. It should be noted that a kind of approximation procedure must be employed to solve the dynamic problems with mixed natural- and constraint-type boundary conditions (Seok et al., 2004). Variational approximation procedure (Tiersten, 1969), which is one of the well-known semi-analytical approximation procedures, is known to be very accurate and simple, but requires obtaining the dispersion relations of the plate in prior to satisfying the remaining equation variationally. In this work, a homogeneous dynamic problem for an infinitely long polarized piezoceramic bimorph plate with two facing edges free is solved by using Hamilton's principle (Lanczos, 1949; Tiersten, 1969) and dispersion relations of the flexural waves propagating to the length direction for the electroded and unelectroded bimorph plate on its major surfaces are derived in the framework of two-dimensional elastoelectricity theory. With further assumptions on electric field quantities, it is shown that reductions on the resulting dispersion relations can be successfully made to a good degree in low frequency range.

2. Derivations of dispersion relations with quasistatic assumptions

2.1. Variational and constitutive equations for piezoceramic bimorph plates

It has been shown that the variational equation of linear piezoelectricity for infinitesimal strain in a volume V bounded by a surface S can be derived from Hamilton's principle and may be written in the form (Tiersten, 1969)

$$\int_{t_0}^{t} \mathrm{d}t \left[\int_V \left[(\tau_{ij,i} + \rho \bar{f}_j - \rho \ddot{u}_j)\delta u_j + D_{k,k}\delta\varphi \right] \mathrm{d}V + \int_{S_N} \left[(\bar{t}_j - n_i\tau_{ij})\delta u_j - (\bar{\sigma} + n_k D_k)\delta\varphi \right] \mathrm{d}S + \int_{S_C} n_i[(u_j - \bar{u}_j)\delta\tau_{ij} + (\varphi - \bar{\varphi})\delta D_i]\,\mathrm{d}S \right] = 0, \tag{1}$$

where S_N, S_C respectively denote the portion of the surface on which natural- and constraint-type conditions are prescribed, ρ represents the reference mass density, ε_{kl}, τ_{ij} respectively represent the components of strain and stress tensor, n_i are the components of the unit outward normal vector of the surface, φ, D_i respectively represent the electric potential and the electric displacement vector, $\bar{t}_j, \bar{f}_j, \bar{u}_j, \bar{\sigma}$ respectively stand for the prescribed traction vector, the prescribed body force density vector, the prescribed displacement vector, the prescribed surface charge. Here we have introduced indicial notation and employed the conventions that repeated tensor indices are to be summed, a comma followed by an index denotes partial differential with respect to a space co-ordinate and a dot over a variable denotes partial differentiation with respect to time.

The constitutive equations relating the elastic field tensors (τ_{ij} and ε_{kl}) and the electric field vectors (E_k and D_i) can be expressed with the following pair of piezoelectric equations (Mason, 1964):

$$\begin{cases} \tau_{ij} = c^E_{ijkl}\varepsilon_{kl} - e_{kij}E_k \\ D_i = e_{ikl}\varepsilon_{kl} + \varepsilon^S_{ik}E_k \end{cases}, \tag{2}$$

where the superscripts E and S respectively stand for the situation of constant electric field intensity and strain; c_{ijkl} denote the elastic stiffnesses; ε_{ik} with superscript are dielectric permittivities; e_{kij} are piezoelectric constants. Even though Eq. (2) is the only form of the constitutive equations which is of any value for the unbounded piezoelectric medium, other three different forms of constitutive equations, [1] although exact, are employed in approximations under certain limiting circumstances; thus any one of these three pairs of constitutive equations are utilized in general when certain variables on the right-hand sides are approximately zero (IEEE std., 1978). Since piezoceramic material is confined to have C_{6v} ($6mm$) symmetry, the constitutive equations in Eq. (2) may be written as a more convenient matrix form with the abbreviated index notation (Mindlin, 1955)

$$\begin{bmatrix} \tau_1 \\ \tau_2 \\ \tau_3 \\ \tau_4 \\ \tau_5 \\ \tau_6 \\ D_1 \\ D_2 \\ D_3 \end{bmatrix} = \begin{bmatrix} c^E_{11} & c^E_{12} & c^E_{13} & 0 & 0 & 0 & 0 & 0 & -e_{31} \\ c^E_{12} & c^E_{11} & c^E_{13} & 0 & 0 & 0 & 0 & 0 & -e_{31} \\ c^E_{13} & c^E_{13} & c^E_{33} & 0 & 0 & 0 & 0 & 0 & -e_{33} \\ 0 & 0 & 0 & c^E_{44} & 0 & 0 & 0 & -e_{15} & 0 \\ 0 & 0 & 0 & 0 & c^E_{44} & 0 & -e_{15} & 0 & 0 \\ 0 & 0 & 0 & 0 & 0 & c_{66} & 0 & 0 & 0 \\ 0 & 0 & 0 & 0 & e_{15} & 0 & \varepsilon^S_{11} & 0 & 0 \\ 0 & 0 & 0 & e_{15} & 0 & 0 & 0 & \varepsilon^S_{11} & 0 \\ e_{31} & e_{31} & e_{33} & 0 & 0 & 0 & 0 & 0 & \varepsilon^S_{33} \end{bmatrix} \begin{bmatrix} \varepsilon_1 \\ \varepsilon_2 \\ \varepsilon_3 \\ \varepsilon_4 \\ \varepsilon_5 \\ \varepsilon_6 \\ E_1 \\ E_2 \\ E_3 \end{bmatrix}, \tag{3}$$

where

$$c_{66} = (c_{11} - c_{12})/2 \tag{4}$$

[1] These four sets of equations are not independent since the constants are related with each other through the coupled thermodynamic relations.

and the elastic properties of the piezoceramic material are polarized along x_3 direction. Note that the number of independent material constants for the above mentioned class of material is 10.

The substitution of Eq. $(3)_3$ into Eqs. $(3)_1$ and $(3)_2$ yields

$$\tau_a - c_{13}^{E^*}\tau_3 = c_{11}^{E^*}\varepsilon_a + c_{12}^{E^*}\varepsilon_{\bar{a}} - e_{31}^{*}E_3, \tag{5}$$

where

$$\bar{a} = 1 \text{ for } a = 2, \quad \bar{a} = 2 \text{ for } a = 1, \ \ a = 1, 2$$

and

$$c_{1a}^{E^*} = c_{1a}^{E} - c_{13}^{E^2}/c_{33}^{E}, \ \ c_{13}^{E^*} = c_{13}^{E}/c_{33}^{E}, \ \ e_{31}^{*} = e_{31} - c_{13}^{E}e_{33}/c_{33}^{E}, \ \ \hat{v} = c_{12}^{E^*}/c_{11}^{E^*}. \tag{6}$$

With the plane stress assumptions along the thickness direction for thin plates, Eq. (5) only contains the stress and strain components in planar directions. Nevertheless, each stress and strain function still has three-dimensional dependencies. In addition, the strain–displacement relations, quasistatic electric field–electric scalar potential relations

$$\varepsilon_{ij} = \tfrac{1}{2}(u_{i,j} + u_{j,i}), \quad E_k = -\varphi_{,k} \tag{7}$$

are required in this description.

As can be seen in Eqs. (5) and (6), the mechanical quantities (stress and strain) are coupled with the mechanical quantities (electric field intensity and electric displacement) through the piezoelectric constants e_{ip}, which will be explained in subsequent sections.

2.2. Dispersion relations of a fully electroded bimorph plate subject to a prescribed voltage

Consider a thin parallel bimorph plate with fully electroded major surfaces on which electric potentials are prescribed. The electric potential φ may be expanded in a series of powers of the thickness co-ordinate x_3 since the thickness is assumed to be much thinner than the other dimensions. A cross-sectional view of a symmetric bimorph plate with fully electroded major surfaces is shown in Fig. 1. The plate is polarized along the x_3 axis, total thickness is $2h$, total width is $2b$, and infinitesimally thin electrodes are attached to the top, bottom and inserted in the middle. Here, the superscripts in the middle denote the layers: (1) for the upper layer and (2) for the lower layer.

Note that the electrodes are assumed to be infinitesimally thin, and thus the effects of the elastic stiffness and inertia of the electrodes are ignored in this description. Since the bimorph plate is comprised of two layers, the electric potential needs to be expanded separately for each layer. In addition, it is assumed that the plate is fully covered with electrodes, so that the potential difference across the electrodes can be independent of the position in the plane of plate even though this assumption can be relaxed with the special expansion adopted here.

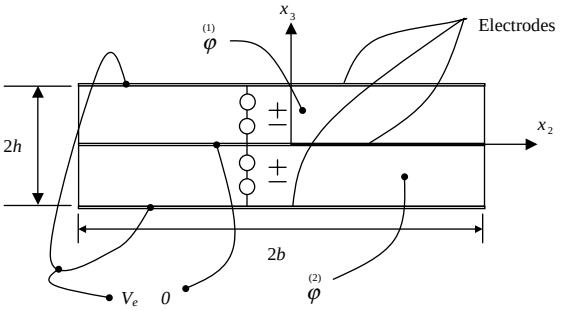

Fig. 1. Cross-sectional view of a fully electroded bimorph plate.

Expansions of the electrical potential functions along the thickness co-ordinate take the form (Seok, 2001)

$$\overset{(m)}{\varphi} = \overset{(m)}{\varphi^{(0)}} + \frac{x_3}{h}\overset{(m)}{\varphi^{(1)}} + \frac{x_3}{h}\left(\frac{x_3}{h} + \hat{m}\right)\overset{(m)}{\varphi^{(2)}}, \quad \hat{m} = (-1)^m, \ \ m = 1, 2, \tag{8}$$

where only the coefficients of $\overset{(1)}{\varphi^{(2)}}$ and $\overset{(2)}{\varphi^{(2)}}$ are set to vanish at the surface of the plate so that those components of potential may vary with position (Tiersten, 1993). This approach allows the variation of the second order component in the electroded region as well as in the unelectroded region, so that the problem may easily be extended to the higher order and/or partially electroded case if this expansion is employed. Such an expansion can give proper differential equations for the partially electroded case in which the first and the second order components of electric potential in the unelectroded region are the functions of position in planar directions as well.

The substitution of Eq. (8) into the electric parts of variational equation, Eq. (1), and the integration of the resulting functions over each layer, after some manipulations including the application of the planar divergence theorem, may yield the electric part of the variational equation for the bimorph plate in the form

$$\begin{aligned}
&\int_{t_0}^{t} \mathrm{d}t \left[\sum_{m=1}^{2} \left[\int_{\hat{S}} \left\{ \left(\overset{(m)}{D^{(0)}_{a,a}} + \overset{(m)}{d^{(0)}_{3}} \right) \delta \overset{(m)}{\varphi^{(0)}} + \frac{1}{h} \left(\overset{(m)}{D^{(1)}_{a,a}} - \overset{(m)}{D^{(0)}_{3}} + \overset{(m)}{d^{(1)}_{3}} \right) \delta \overset{(m)}{\varphi^{(1)}} \right.\right.\right. \\
&\quad \left. + \frac{1}{h^2} \left(\overset{(m)}{D^{(2)}_{a,a}} + \hat{m}h \overset{(m)}{D^{(1)}_{a,a}} - 2\overset{(m)}{D^{(1)}_{3}} - \hat{m}h \overset{(m)}{D^{(0)}_{3}} \right) \delta \overset{(m)}{\varphi^{(2)}} \right\} \mathrm{d}S \\
&\quad - \int_{\overset{(m)}{C_N}} \mathrm{d}s \left[\frac{1}{h} \left(\overset{(m)}{\bar{\sigma}^{(1)}} + n_a \overset{(m)}{D^{(1)}_{a}} \right) \delta \overset{(m)}{\varphi^{(1)}} + \frac{1}{h^2} \left\{ \left(\overset{(m)}{\bar{\sigma}^{(2)}} + n_a \overset{(m)}{D^{(2)}_{a}} \right) + \hat{m}h \left(\overset{(m)}{\bar{\sigma}^{(1)}} + n_a \overset{(m)}{D^{(1)}_{a}} \right) \right\} \delta \overset{(m)}{\varphi^{(2)}} \right] + \Psi \Bigg],
\end{aligned} \tag{9}$$

where

$$\begin{aligned}
\Psi = \int_{\hat{S}} \Bigg[&\left[\left[\left(\overset{(2)}{\varphi^{(0)}} - \overset{(2)}{\bar{\varphi}^{(0)}} \right) \delta D_3 \right]_{x_3=0^-} - \left[\left(\overset{(1)}{\varphi^{(0)}} - \overset{(1)}{\bar{\varphi}^{(0)}} \right) \delta D_3 \right]_{x_3=0^+} \right. \\
&+ \left[\left\{ \left(\overset{(1)}{\varphi^{(0)}} - \overset{(1)}{\bar{\varphi}^{(0)}} \right) + \left(\overset{(1)}{\varphi^{(1)}} - \overset{(1)}{\bar{\varphi}^{(1)}} \right) \right\} \delta D_3 \right]_{x_3=h} \\
&\left. - \left[\left\{ \left(\overset{(2)}{\varphi^{(0)}} - \overset{(2)}{\bar{\varphi}^{(0)}} \right) - \left(\overset{(2)}{\varphi^{(1)}} - \overset{(2)}{\bar{\varphi}^{(1)}} \right) \right\} \delta D_3 \right]_{x_3=-h} \mathrm{d}S \Bigg],
\end{aligned} \tag{10}$$

$$\overset{(m)}{d^{(n)}_{3}} = \left\{ \begin{array}{ll} [D_3 x_3^n]_0^h & \text{for } m = 1 \\ [D_3 x_3^n]_{-h}^0 & \text{for } m = 2 \end{array} \right\}, \quad n = 0, 1 \tag{11}$$

and $\hat{S}$ denotes the major surfaces of the plate, and $\overset{(m)}{C_N}$ stands for the edges of the mth layer on which natural-types of boundary conditions are prescribed.

In addition, the superscript on the right-hand side of each symbol denotes the order of the component expanded, and

$$\overset{(1)}{D^{(n)}_{j}} = \int_0^h D_j x_3^n \, \mathrm{d}x_3, \quad \overset{(2)}{D^{(n)}_{j}} = \int_{-h}^0 D_j x_3^n \, \mathrm{d}x_3 \tag{12}$$

are defined as the nth order components of electric displacement.

Using Eqs. (9) and (10), the charge equations of electrostatics with the prescribed electric potentials for the two-dimensional bimorph plate may be obtained in the form

$$\oint_{\overset{(m)}{C}} n_a \overset{(m)}{D_a^{(1)}}\,\mathrm{d}s - \int_S \overset{(m)}{D_3^{(0)}}\,\mathrm{d}S + \int_S \overset{(m)}{d_3^{(1)}}\,\mathrm{d}S = 0, \tag{13}$$

$$\overset{(m)}{D_{a,a}^{(2)}} + \hat{m}h\overset{(m)}{D_{a,a}^{(1)}} - 2\overset{(m)}{D_3^{(1)}} - \hat{m}h\overset{(m)}{D_3^{(0)}} = 0, \tag{14}$$

$$\overset{(m)}{\varphi^{(n)}} = \overset{(m)}{\bar{\varphi}^{(n)}}, \quad m = 1,2, \ \ n = 0,1, \tag{15}$$

where $\overset{(m)}{C}$ is the prismatic contour of edges of the mth layer.

For convenience, let us set

$$\overset{(m)}{\bar{\varphi}^{(0)}} = 0, \quad \overset{(m)}{\bar{\varphi}^{(1)}} = -\hat{m}V_{\mathrm{e}}, \tag{16}$$

where V_{e} means the voltage and designates the potential difference between the top (or bottom) electrode and the electrode in the middle.

Note that Eq. (13) contains integral conditions over the two pairs of electrodes, and simply express algebraic equations. This is because the first component of the electric potential function is independent of position in the planar directions, so that the variation of that component should be pulled out from the integration in the variational equation. Therefore, if voltage V_{e} is prescribed, the conditions in Eq. (13) merely serve to determine the current through the electrodes (Tiersten, 1993). On the other hand, if voltage V_{e} is not prescribed, these conditions are needed in order to obtain solutions because the relations between deflection (or slope) and the induced voltage (or current) can be obtained.

Considering the fact that the shear stress is not coupled to the electric quantities, the planar shear strain for thin plates, with the strain–displacement relations, Eq. $(7)_1$, leads to

$$\varepsilon_{12} = \frac{1}{2}\sum_{n=0}^{1} x_3^n(u_{1,2}^{(n)} + u_{2,1}^{(n)}) = \sum_{n=0}^{1} x_3^n e_{12}^{(n)}, \tag{17}$$

where

$$\varepsilon_{12}^{(0)} = \frac{1}{2}\left(u_{1,2}^{(0)} + u_{2,1}^{(0)}\right), \quad \varepsilon_{12}^{(1)} = \frac{1}{2}\left(u_{1,2}^{(1)} + u_{2,1}^{(1)}\right) = -u_{3,12}^{(0)}. \tag{18}$$

The insertion of Eq. (17) in the constitutive equation for shear stress τ_{12} yields

$$\tau_{12} = 2c_{66}\varepsilon_{12} = 2c_{66}\left\{\frac{1}{2}\left(u_{1,2}^{(0)} + u_{2,1}^{(0)}\right) - x_3 u_{3,12}^{(0)}\right\}. \tag{19}$$

Multiplying x_3^n and integrating over the thickness, we obtain the nth order components of the shear stress in the form

$$\tau_{12}^{(n)} = \int_{-h}^{h} \tau_{12} x_3^{(n)}\,\mathrm{d}x_3 = c_{66}\left\{\left[\frac{x_3^{n+1}}{n+1}\right]_{-h}^{h}\left(u_{1,2}^{(0)} + u_{2,1}^{(0)}\right) - 2\left[\frac{x_3^{n+2}}{n+2}\right]_{-h}^{h} u_{3,12}^{(0)}\right\}. \tag{20}$$

Thus, the zeroth and the first component of the shear stress can readily be obtained through the use of Eq. (19) as

$$\tau_{12}^{(0)} = 2c_{66}h\left(u_{1,2}^{(0)} + u_{2,1}^{(0)}\right), \quad \tau_{12}^{(1)} = -2\tilde{D}u_{3,12}^{(0)}, \tag{21}$$

where

$$\tilde{D} = 2h^3 c_{66}/3. \tag{22}$$

With the additional relation in the material with transversely isotropy, [2] Eq. (4), written in a different form

$$c_{66} = c_{11}^{E^*}(1-\hat{v})/2. \tag{23}$$

Eq. $(21)_2$ can simply be seen to result in

$$\tau_{12}^{(1)} = -\hat{D}(1-\hat{v})u_{3,12}^{(0)}. \tag{24}$$

For the systematic development of the linear equations with electric quantities, it may be necessary to couple the electric potentials expanded in series to the mechanical quantities. For the sake of brevity, series expansions of mechanical stress and electric displacement resultants are developed and explained in Appendix A.

The substitution of Eq. (8) into Eq. $(7)_2$, and then into Eqs. (A.4) combined with Eq. (16), yields the components of electric displacement resultants for the zeroth order

$$\overset{(m)}{D}{}_3^{(0)} = \hat{m}\varepsilon_{33}^{S^*}V_{\mathrm{e}} + e_{31}^*\left(h\varepsilon_{aa}^{(0)} - \hat{m}\frac{h^2}{2}\varepsilon_{aa}^{(1)}\right) \tag{25}$$

and for the first order

$$\overset{(m)}{D}{}_3^{(1)} = -\frac{\varepsilon_{33}^{S^*}}{2}h\left(V_{\mathrm{e}} + \frac{1}{3}\overset{(m)}{\varphi}{}^{(2)}\right) - e_{31}^*\left(\hat{m}\frac{h^2}{2}\varepsilon_{aa}^{(0)} - \frac{h^3}{3}\varepsilon_{aa}^{(1)}\right) \tag{26}$$

along with the electric field intensity components in the thickness co-ordinate

$$\overset{(m)}{E}_3 = \sum_{n=0}^{1} x_3^n \overset{(m)}{E}_3^{(n)}, \tag{27}$$

where

$$\overset{(m)}{E}_3^{(0)} = \frac{\hat{m}}{h}\left(V_{\mathrm{e}} - \overset{(m)}{\varphi}{}^{(2)}\right), \quad \overset{(m)}{E}_3^{(1)} = -\frac{2}{h^2}\overset{(m)}{\varphi}{}^{(2)}. \tag{28}$$

The insertion of Eqs. (27), (28) in Eq. (A.3) combined with the two-dimensional strain–displacement relations and the use of symmetry of bimorph with $\varphi^{(2)} = \overset{(m)}{\varphi}{}^{(2)}$ for $m = 1, 2$ yields the moment resultants in the form

$$\tau_a^{(1)} = e_{31}^* h(V_{\mathrm{e}} + \varphi^{(2)}/3) - \hat{D}(u_{3,a(a)}^{(0)} + \hat{v}u_{3,\bar{a}(\bar{a})}^{(0)}), \tag{29}$$

where

$$\hat{D} = 2h^3 c_{11}^{E^*}/3 \tag{30}$$

and we have introduced the series expansion of mechanical displacement along the thickness co-ordinate (Seok et al., 2004)

$$u_j = u_j^{(0)} + u_j^{(1)}x_3 + u_j^{(2)}\delta_{j3}x_3^2. \tag{31}$$

[2] Piezoceramics used in this work have the symmetry of 6*mm* (Mason, 1964), hence exhibits transversely isotropy, where the number of independent components in the elastic stiffness tensor is reduced to 5.

The shear stress components can be obtained from the similar manner in the form

$$\tau_{3a}^{(0)} + \tau_{12,\bar{a}}^{(1)} = -\hat{D}\left[\left\{u_{3,a(a)(a)}^{(0)} + (2-\hat{v})u_{3,a(\bar{a})(\bar{a})}^{(0)}\right\} + \frac{h}{3}\tilde{e}_{31}^{*}\varphi_{,a}^{(2)}\right], \tag{32}$$

where we have used the relation $\tau_{3a}^{(0)} = \tau_{ab,b}^{(1)}$, which is Eq. (17b) of Seok et al. (2004), instead of constitutive equations for the thin plates and defined a new parameter

$$\tilde{e}_{31}^{*} = e_{31}^{*}/\hat{D}. \tag{33}$$

The substitution of Eqs. (29) and $(21)_2$ into Eq. (18) of Seok et al. (2004)

$$\tau_{ab,ab}^{(1)} = 2\rho h\ddot{w} \tag{34}$$

and the replacement of $u_3^{(0)}$ by w for notational convenience yields the governing differential equation of displacement coupled with electric potential in the from

$$\hat{w}_{,1111} + 2\hat{w}_{,1122} + \hat{w}_{,2222} - \hat{\kappa}^2\omega^2\hat{w} - \frac{h}{3}\tilde{e}_{31}^{*}\hat{\varphi}_{,aa}^{(2)} = 0, \tag{35}$$

where

$$w = \hat{w}(x_a)\mathrm{e}^{\mathrm{i}\omega t}, \quad \varphi^{(2)} = \hat{\varphi}^{(2)}(x_a)\mathrm{e}^{\mathrm{i}\omega t}, \quad \hat{\kappa}^2 = 2\rho h/\hat{D}. \tag{36}$$

Using Eqs. (14), (A.8) and (A.9), the differential equation for $\overset{(m)}{\varphi}{}^{(2)}$ can be obtained in the form

$$\overset{(m)}{\varphi}{}_{,aa}^{(2)} - \frac{10}{h^2}\hat{\varepsilon}_{33}^{S^*}\overset{(m)}{\varphi}{}^{(2)} + 5\hat{e}_{31}^{*}\varepsilon_{aa}^{(1)} = 0, \tag{37}$$

where

$$\hat{\varepsilon}_{33}^{S^*} = \varepsilon_{33}^{S^*}/\varepsilon_{11}^{S^*}, \quad \hat{e}_{31}^{*} = e_{31}^{*}/\varepsilon_{11}^{S^*}. \tag{38}$$

Through the use of Eqs. (A.2), (31) and the plane stress assumptions, Eq. (37) can be re-written in the form

$$\varphi_{,aa}^{(2)} - \frac{10}{h^2}\hat{\varepsilon}_{33}^{S^*}\varphi^{(2)} - 5\hat{e}_{31}^{*}w_{,aa} = 0. \tag{39}$$

The substitution of

$$[\hat{w}, \hat{\varphi}^{(2)}]^{\mathrm{T}} = [\tilde{w}, \tilde{\varphi}^{(2)}]^{\mathrm{T}}\mathrm{e}^{-\mathrm{i}(\xi x_1 + \eta x_2)} \tag{40}$$

into Eqs. (35) and (39) enables to yield the dimensionless form of coupled homogeneous equation

$$\begin{bmatrix} \bar{\eta}^2 + \bar{\xi}^2 + 10\bar{\hat{\varepsilon}}_{33}^{S^*} & 5\hat{e}_{31}^{S^*}(\bar{\eta}^2 + \bar{\xi}^2) \\ \bar{\tilde{e}}_{31}^{S^*}(\bar{\eta}^2 + \bar{\xi}^2) & 3\left(\bar{\eta}^4 + 2\bar{\eta}^2\bar{\xi}^2 + \bar{\xi}^4 - \bar{\kappa}^2\bar{\Omega}^2\right) \end{bmatrix} \begin{bmatrix} \tilde{\varphi}^{(2)} \\ \tilde{w} \end{bmatrix} = \begin{bmatrix} 0 \\ 0 \end{bmatrix}, \tag{41}$$

with the amplitude ratios

$$\bar{\tilde{w}} = \bar{\eta}^2 + \bar{\xi}^2 + 10\bar{\hat{\varepsilon}}_{33}^{S^*}, \quad \bar{\tilde{\varphi}}^{(2)} = -5\hat{e}_{31}^{S^*}(\bar{\eta}^2 + \bar{\xi}^2), \tag{42}$$

where the dimensionless parameters

$$\begin{aligned} &\bar{\kappa} = (2b/\pi)^2\hat{\kappa}\bar{\omega}, \quad \bar{\hat{\varepsilon}}_{33}^{S^*} = (2b)^2/(\pi h)^2\hat{\varepsilon}_{33}^{S^*}, \quad \bar{\tilde{e}}_{31}^{*}\frac{2b}{\pi h}\tilde{e}_{31}^{*}, \quad \bar{\eta} = 2b\eta/\pi, \quad \bar{\xi} = 2b\xi/\pi, \\ &\bar{\omega} = \pi\sqrt{c_{66}/\rho}/(2b), \quad \bar{\Omega} = \omega/\bar{\omega}, \quad \bar{x}_a = \pi x_a/(2b), \quad \tau = \bar{\omega}t \end{aligned} \tag{43}$$

have been newly introduced.

Being cubic in $\bar{\eta}^2$, the vanishing determinant of Eq. (41) gives three $\bar{\eta}$'s ($\bar{\eta}_k,\ k = 1,\ldots,3$) with three amplitude ratios of $\tilde{\varphi}^{(2)}$ vs. $\tilde{w}$ ($\bar{\tilde{\varphi}}_k^{(2)} : \bar{\tilde{w}}_k,\ k = 1,\ldots,3$) for a given $\bar{\Omega}$ and $\bar{\xi}$. After dispensing with the unsymmetrical part of the solution for $\hat{w}$ and $\hat{\varphi}^{(2)}$ in Eq. (40), the solution functions become

$$\hat{\varphi}^{(2)}(\bar{x}_a) = \sum_{k=1}^{3} A_k \bar{\tilde{\varphi}}_k^{(2)} \cos(\bar{\eta}_k \bar{x}_2) \mathrm{e}^{-\mathrm{i}\bar{\xi}\bar{x}_1}, \tag{44}$$

$$\hat{w}(\bar{x}_a) = \sum_{k=1}^{3} A_k \bar{\tilde{w}}_k \cos(\bar{\eta}_k \bar{x}_2) \mathrm{e}^{-\mathrm{i}\bar{\xi}\bar{x}_1}, \tag{45}$$

where A_k are constants to be determined and summation convention for the repeated indices has been suppressed. In this equation the functions $\hat{\varphi}^{(2)}(x_a)$, $\hat{w}(x_a)$ have been directly replaced by new functions $\hat{\varphi}^{(2)}(\bar{x}_a)$, $\hat{w}(\bar{x}_a)$, which for corresponding points x_a and $\bar{x}_a$ have the same values as the former function and for the sake of simplicity are denominated by the same symbols. This simplification will be understood throughout this work. It should be noted that the symmetric excitation of a bimorph plate only permits the symmetric modes for the flexural vibration with respect to the $\bar{x}_1$ axis.

Three pairs of boundary conditions at the two side-edges required in deriving the dispersion relations are vanishing electric displacement as well as vanishing moments and shear forces. The application of the solution functions in Eqs. (44) and (45) to the two boundary conditions with zero voltage on the electrodes yields

$$\sum_{i=1}^{3} A_i \left\{ 3\left(\bar{\eta}_i^2 + \hat{\nu}\bar{\xi}^2\right)\bar{\tilde{w}}_i + \bar{\tilde{e}}_{31}^{*}\bar{\tilde{\varphi}}_i^{(2)} \right\} \cos(\pi\bar{\eta}_i/2) = 0, \tag{46}$$

$$\sum_{i=1}^{3} A_i \left[3\left\{ \bar{\eta}_i^2 + (2-\hat{\nu})\bar{\xi}^2 \right\}\bar{\eta}_i\bar{\tilde{w}}_i + \bar{\tilde{e}}_{31}^{*}(\bar{\eta}_i^2 + \bar{\xi}^2)\bar{\eta}_i\bar{\tilde{\varphi}}_i^{(2)} \right] \sin(\pi\bar{\eta}_i/2) = 0, \tag{47}$$

$$\sum_{i=1}^{3} A_i \bar{\tilde{e}}_{31}^{*}\bar{\eta}_i\bar{\tilde{\varphi}}_i^{(2)} \sin(\pi\bar{\eta}_i/2) = 0. \tag{48}$$

Eqs. (46)–(48) compose a 3 by 3 homogeneous matrix equation with one unknown solution vector composed of three A's as its components. The vanishing determinant gives the dispersion relations, which yields the solution functions, with the inclusion of N dispersion branches, in the form

$$\hat{w}(\bar{x}_a) = \sum_{i=1}^{N}\sum_{j=1}^{3}\sum_{k=1}^{2} B_{ik}\bar{\tilde{w}}_{ij}\bar{A}_{ij} \cos(\bar{\eta}_{ij}\bar{x}_2) \sin\{\bar{\xi}_i\bar{x}_1 + (k-1)\pi/2\}, \tag{49}$$

$$\hat{\varphi}^{(2)}(\bar{x}_a) = \sum_{i=1}^{N}\sum_{j=1}^{3}\sum_{k=1}^{2} B_{ik}\bar{\tilde{\varphi}}_{ij}^{(2)}\bar{A}_{ij} \cos(\bar{\eta}_{ij}\bar{x}_2) \sin\{\bar{\xi}_i\bar{x}_1 + (k-1)\pi/2\}, \tag{50}$$

where

$$F_{ij} = F_j(\bar{\xi}_i), \quad F = \bar{A}, \bar{\tilde{w}}, \bar{\eta}, \quad \text{and} \quad \bar{\tilde{\varphi}}^{(2)},\ n = 1,2 \tag{51}$$

and B_{ik} are constants to be determined.

The relations between the mechanical quantities and the electric potential, which is prescribed on the electrodes attached to the major surfaces and inserted in the middle plane, have been derived in this section. However, if the electric potentials are not prescribed on the electrodes, the relations between the deforma-

tion and the induced electrical quantities should be obtained so as to measure the deformation of the plate quantitatively, which is derived and explained in Appendix B.

2.3. Dispersion relations of a unelectroded bimorph plate

For the unelectroded plate, a part of the electric boundary conditions, which is denoted as Ψ in Eq. (9), should be replaced by

$$\Psi = \int_{\hat{S}} \mathrm{d}S \left[\left[\overset{(1)}{\bar{\sigma}} + \overset{(1)}{D}_3 \right]_{x_3=h} \delta\left(\overset{(1)}{\varphi^{(0)}} + \overset{(1)}{\varphi^{(1)}} \right) + \left[\overset{(1)}{\bar{\sigma}} - \overset{(1)}{D}_3 \right]_{x_3=0^+} \delta \overset{(1)}{\varphi^{(0)}} + \left[\overset{(2)}{\bar{\sigma}} - \overset{(2)}{D}_3 \right]_{x_3=-h} \delta\left(\overset{(2)}{\varphi^{(0)}} - \overset{(2)}{\varphi^{(1)}} \right) + \left[\overset{(2)}{\bar{\sigma}} + \overset{(2)}{D}_3 \right]_{x_3=0^-} \delta \overset{(2)}{\varphi^{(0)}} \right]. \tag{52}$$

Furthermore, the integral conditions in Eq. (13) for the fully electroded case must be changed to

$$\overset{(m)}{D}{}^{(1)}_{a,a} - \overset{(m)}{D}{}^{(0)}_{3} = 0, \tag{53}$$

where the condition $\overset{(m)}{d}{}^{(1)}_{3} = 0$ has already been introduced since $D_3(x_3 = \pm h) = 0$ and the central electrode is assumed to be earthed. The other two differential equations required in this description are Eqs. (14) and (34).

Using Eqs. (A.4) together with Eq. (8), the electric displacement components in the x_3 direction can be obtained in the form

$$\overset{(m)}{D}{}^{(0)}_{3} = -\varepsilon^{S^*}_{33} \overset{(m)}{\varphi^{(1)}} - \hat{m} \frac{e^*_{31} h^2}{2} \varepsilon^{(1)}_{aa}, \tag{54}$$

$$\overset{(m)}{D}{}^{(1)}_{3} = \frac{\varepsilon^{S^*}_{33} h}{2} \left(\hat{m} \overset{(m)}{\varphi^{(1)}} - \frac{1}{3} \overset{(m)}{\varphi^{(2)}} \right) + \frac{e^*_{31} h^3}{3} \varepsilon^{(1)}_{aa}, \tag{55}$$

since

$$\overset{(m)}{E}_3 = -\frac{1}{h} \left(\overset{(m)}{\varphi^{(1)}} + \hat{m} \overset{(m)}{\varphi^{(2)}} \right) - 2 \frac{x_3}{h} \overset{(m)}{\varphi^{(2)}}. \tag{56}$$

Through the use of Eqs. (8) and (A.8), the nth order components of electric displacement in the plane directions can be obtained in the form

$$\overset{(m)}{D}{}^{(n)}_{a} = \hat{m} \left\{ \left(\overset{(m)}{\varphi^{(1)}_{,a}} + \hat{m} \overset{(m)}{\varphi^{(2)}_{,a}} \right) \frac{(-\hat{m}h)^{n+2}}{n+2} + \frac{1}{h} \overset{(m)}{\varphi^{(2)}_{,a}} - \frac{(-\hat{m}h)^{n+3}}{n+3} \right\}, \quad n = 0, \ldots, 2. \tag{57}$$

With the aid of Eqs. (56) and (A.3), the moment resultants can be obtained as

$$\tau^{(1)}_{a} = \sum_{m=1}^{2} \overset{(m)}{\tau^{(1)}_{a}} = \frac{2}{3} h^3 c^{E^*}_{11} (\varepsilon^{(1)}_{a} + \hat{v} \varepsilon^{(1)}_{\bar{a}}) + \frac{h}{2} e^*_{31} \left\{ \left(\overset{(1)}{\varphi^{(1)}} - \overset{(2)}{\varphi^{(1)}} \right) + \frac{1}{3} \left(\overset{(1)}{\varphi^{(2)}} - \overset{(2)}{\varphi^{(2)}} \right) \right\}. \tag{58}$$

Through the use of the symmetry of the bimorph plate with respect to the middle plane, i.e., $\overset{(2)}{\varphi^{(1)}} = -\overset{(1)}{\varphi^{(1)}}$, $\overset{(2)}{\varphi^{(2)}} = \overset{(1)}{\varphi^{(2)}}$, Eq. (53), combined with Eq. (57), may lead to

$$\varphi^{(1)}_{,aa} - \frac{1}{4} \varphi^{(2)}_{,aa} - \frac{3}{h^2} \hat{\varepsilon}^{S^*}_{33} \varphi^{(1)} - \frac{3}{2} \hat{e}^*_{31} w_{,aa} = 0. \tag{59}$$

Similarly, Eq. (14) yields the second differential equation for the electric potential components coupled with the mechanical displacement of the plate in the form

$$\frac{5}{2}\varphi^{(1)}_{,aa} - \varphi^{(2)}_{,aa} + \frac{10}{h^2}\hat{\varepsilon}^{S^*}_{33}\varphi^{(2)} + 5\hat{e}^*_{31}w_{,aa} = 0. \tag{60}$$

The third differential equation can be easily obtained from Eqs. (24), (34) and (58), after ignoring all body forces and moments, with the result

$$w_{,1111} + 2w_{,1122} + w_{,2222} + \hat{\kappa}^2\ddot{w} - \frac{h}{3}\tilde{e}^*_{31}(3\varphi^{(1)}_{,aa} + \varphi^{(2)}_{,aa}) = 0. \tag{61}$$

By letting the solutions of the three coupled differential equations (59)–(61) as

$$\varphi^{(n)} = \tilde{\varphi}^{(n)}\mathrm{e}^{\mathrm{i}(\omega t - \xi x_1 - \eta x_2)}, \quad n = 1, 2, \tag{62}$$

$$w = \tilde{w}\mathrm{e}^{\mathrm{i}(\omega t - \xi x_1 - \eta x_2)} \tag{63}$$

a set of homogeneous equations for the three coupled quantities can be obtained as the following matrix equation with dimensionless quantities defined in Eq. (43):

$$\begin{bmatrix} 10\bar{\hat{\varepsilon}}^{S^*}_{33} + \frac{10}{3}(\bar{\eta}^2 + \bar{\xi}^2) & -\frac{5}{6}(\bar{\eta}^2 + \bar{\xi}^2) & -5\hat{e}^*_{31}(\bar{\eta}^2 + \bar{\xi}^2) \\ \frac{5}{2}(\bar{\eta}^2 + \bar{\xi}^2) & -\left\{10\bar{\hat{\varepsilon}}^{S^*}_{33} + \frac{5}{2}(\bar{\eta}^2 + \bar{\xi}^2)\right\} & 5\hat{e}^*_{31}(\bar{\eta}^2 + \bar{\xi}^2) \\ \bar{\tilde{e}}^*_{31}(\bar{\eta}^2 + \bar{\xi}^2) & \frac{1}{3}\bar{\tilde{e}}^*_{31}(\bar{\eta}^2 + \bar{\xi}^2) & \bar{\eta}^4 + 2\bar{\xi}^2\bar{\eta}^2 + \bar{\xi}^4 - \bar{\kappa}^2\bar{\Omega}^2 \end{bmatrix} \begin{bmatrix} \tilde{\varphi}^{(1)} \\ \tilde{\varphi}^{(2)} \\ \tilde{w} \end{bmatrix} = \begin{bmatrix} 0 \\ 0 \\ 0 \end{bmatrix}. \tag{64}$$

Being quartic in $\bar{\eta}^2$, the vanishing determinant of Eq. (64) yields four $\bar{\eta}$'s ($\bar{\eta}_k,\ k = 1, \ldots, 4$) and the amplitude ratios associated with $\tilde{\varphi}^{(1)}$, $\tilde{\varphi}^{(2)}$, and $\tilde{w}$ ($\bar{\tilde{\varphi}}^{(1)}_k : \bar{\tilde{\varphi}}^{(2)}_k : \bar{\tilde{w}}_k,\ k = 1, \ldots, 4$) in the way explained in the previous section for a given $\bar{\Omega}$ and $\bar{\xi}$. If the matrix in Eq. (64) is denoted by $\mathbf{M}$ with its components M_{ij}, $i,j = 1, \ldots, 3$, one obtains

$$\bar{\tilde{\varphi}}^{(1)}_k = L_{\gamma 1}(\bar{\eta}_k), \quad \bar{\tilde{\varphi}}^{(2)}_k = L_{\gamma 2}(\bar{\eta}_k), \quad \bar{\tilde{w}}_k = L_{\gamma 3}(\bar{\eta}_k), \ \ k = 1, \ldots, 4, \tag{65}$$

where

$$L_{pq}(\bar{\eta}_k) = \mathrm{cof}\{M_{pq}(\bar{\eta} = \bar{\eta}_k)\}, \quad p, q = 1, \ldots, 3, \ \ k = 1, \ldots, 4 \tag{66}$$

and γ can be any number between 1 and 3. In Eq. (66) cof{ } represents a cofactor of the argument matrix. Hence, the solution functions with the dimensionless arguments may be represented as

$$\varphi^{(n)}(\bar{x}_a, \tau) = \sum_{k=1}^{4} A_k \bar{\tilde{\varphi}}^{(n)}_k \cos(\bar{\eta}_k \bar{x}_2)\mathrm{e}^{\mathrm{i}(\bar{\Omega}\tau - \bar{\xi}\bar{x}_1)}, \tag{67}$$

$$w(\bar{x}_a, \tau) = \sum_{k=1}^{4} A_k \bar{\tilde{w}}_k \cos(\bar{\eta}_k \bar{x}_2)\mathrm{e}^{\mathrm{i}(\bar{\Omega}\tau - \bar{\xi}\bar{x}_1)}, \tag{68}$$

where $\bar{\tilde{\varphi}}^{(n)}_k$, $\bar{\tilde{w}}_k$ are amplitude ratios obtained from Eq. (64) and A_k are unknown amplitudes to be determined. It should also be noticed that the functions $\varphi^{(2)}(x_a, t)$, $w(x_a, t)$ were directly replaced by new functions $\varphi^{(2)}(\bar{x}_a, \tau)$, $w(\bar{x}_a, \tau)$, which for corresponding points (x_a, t) and $(\bar{x}_a, \tau)$ have the same values as the former function and are denominated by the same symbols for convenience. This simplification will also be understood in this section.

The application of Eqs. (67) and (68) to the homogeneous constraint-type edge conditions gives the following four homogeneous equations composing a 4 by 4 matrix equation, which gives dispersion relations and amplitude ratios for the four A's:

$$\sum_{i=1}^{4} A_i \left\{ \left(\bar{\eta}_i^2 + \hat{v}\bar{\bar{\xi}}^2 \right) \bar{\bar{w}}_i + \bar{\bar{e}}_{31}^{*} \left(3\bar{\bar{\varphi}}_i^{(1)} + \bar{\bar{\varphi}}_i^{(2)} \right) \Big/ 3 \right\} \cos(\pi\bar{\eta}_i/2) = 0, \tag{69}$$

$$\sum_{i=1}^{4} A_i \left[\left\{ \bar{\eta}_i^2 + (2-\hat{v})\bar{\bar{\xi}}^2 \right\} \bar{\eta}_i \bar{\bar{w}}_i + \bar{\bar{e}}_{31}^{*} \bar{\eta}_i \left(3\bar{\bar{\varphi}}_i^{(1)} + \bar{\bar{\varphi}}_i^{(2)} \right) \Big/ 3 \right] \sin(\pi\bar{\eta}_i/2) = 0, \tag{70}$$

$$\sum_{i=1}^{4} A_i \bar{\eta}_i \bar{\bar{\varphi}}_i^{(1)} \sin(\pi\bar{\eta}_i/2) = 0, \tag{71}$$

$$\sum_{i=1}^{4} A_i \bar{\eta}_i \bar{\bar{\varphi}}_i^{(2)} \sin(\pi\bar{\eta}_i/2) = 0. \tag{72}$$

Finally the solution functions including N dispersion branches can be represented in the form

$$\varphi^{(n)}(\bar{x}_a, \tau) = \sum_{j=1}^{N} \sum_{k=1}^{4} \sum_{l=1}^{2} B_{jl} \bar{A}_{jk} \bar{\bar{\varphi}}_{jk}^{(n)} \cos(\bar{\eta}_{jk}\bar{x}_2) \sin\{\bar{\bar{\xi}}_j \bar{x}_1 + (l-1)\pi/2\} e^{i\bar{\Omega}\tau}, \tag{73}$$

$$w(\bar{x}_a, \tau) = \sum_{j=1}^{N} \sum_{k=1}^{4} \sum_{l=1}^{2} B_{jl} A_{jk} \bar{\bar{w}}_{jk} \cos(\bar{\eta}_{jk}\bar{x}_2) \sin\{\bar{\bar{\xi}}_j \bar{x}_1 + (l-1)\pi/2\} e^{i\bar{\Omega}\tau}, \tag{74}$$

where B_{ik} are constants to be determined.

3. Reductions of the dispersion relations with the assumptions on electric field quantities

The inclusion of the differential equations for the electric potential components increases the number of functions being evaluated and the matrix size for the analysis of the bounded plate. One may have difficulties in computation if the system has too many components to analyze, hence, requires too many unknown amplitudes to solve. That is because the largest imaginary wave number actually governs the accuracy of the calculated results. Thus, further reduction of the governing equations may be necessary, if possible, for the system interested in this work. This can be done if some small errors produced by neglecting the variations of the electric field intensity along the position in the plane of the plate are permitted. In the two subsequent sections, the procedures to reduce the differential equations for the components of electric potential to the degenerate ones are explained for fully electroded and unelectroded cases separately.

3.1. Reduction of the fully electroded bimorph plate equation

First consider the assumptions that the electrodes fully cover the surfaces of the entire plate with a prescribed voltage and the plate is thin enough to allow for the ignorance of the variations of electric field intensity in the planar directions, i.e., $E_a = 0$, throughout the plate. With these assumptions, the constitutive equations simply give $D_a = 0$ for both layers. Then all that remains in Eq. (14) may become

$$-\hat{m}h \overset{(m)}{D}{}_3^{(0)} - 2 \overset{(m)}{D}{}_3^{(1)} = 0 \tag{75}$$

together with

$$\overset{(m)}{\varphi} = -\hat{m}\frac{x_3}{h} V_e + \frac{x_3}{h}\left(\frac{x_3}{h} + \hat{m}\right) \overset{(m)}{\varphi}{}^{(2)}, \tag{76}$$

which can be obtained from Eqs. (8), (15) and (16). The substitution of Eqs. (25) and (26) into Eq. (75) gives the second components of potential functions in the form

$$\overset{(m)}{\varphi}{}^{(2)} = h^2 e_{31}^* \varepsilon_{aa}^{(1)}/(2\varepsilon_{33}^{S^*}), \quad m = 1, 2, \tag{77}$$

as was expected by virtue of the symmetry of the bimorph plate. Hence the substitution of Eq. (77) into Eq. (8) and then into Eqs. (27) and (28) yields

$$\overset{(m)}{\varphi} = -\hat{m}\frac{x_3}{h}V_e + \frac{x_3}{h}\left(\frac{x_3}{h} + \hat{m}\right)\frac{h^2 e_{31}^*}{2\varepsilon_{33}^{S^*}}\varepsilon_{aa}^{(1)}, \tag{78}$$

$$\overset{(m)}{E}_3 = \hat{m}\left(\frac{V_e}{h} - \frac{h e_{31}^*}{2\varepsilon_{33}^{S^*}}\varepsilon_{aa}^{(1)}\right) - x_3\frac{e_{31}^*}{\varepsilon_{33}^{S^*}}\varepsilon_{aa}^{(1)}. \tag{79}$$

The substitution of Eqs. (78) and (79) into Eq. (A.1), and the rearrangement of the resulting equations yields

$$\tau_a^{(0)} = \sum_{m=1}^{2}\overset{(m)}{\tau}{}_a^{(0)} = 2hc_{11}^{E^*}\left(\varepsilon_a^{(0)} + \hat{\nu}\varepsilon_{\bar{a}}^{(0)}\right), \tag{80}$$

$$\tau_a^{(1)} = \sum_{m=1}^{2}\overset{(m)}{\tau}{}_a^{(1)} = \hat{K}V_e + \bar{\hat{D}}\left(\varepsilon_a^{(1)} + \bar{\hat{\nu}}\varepsilon_{\bar{a}}^{(1)}\right), \tag{81}$$

where

$$\bar{\hat{D}} = \frac{2h^3}{3}\left(c_{11}^{E^*} + \frac{e_{31}^{*2}}{4\varepsilon_{33}^{S^*}}\right), \quad \bar{\hat{\nu}} = \frac{4c_{11}^{E^*}\hat{\nu} + e_{31}^{*2}/\varepsilon_{33}^{S^*}}{4c_{11}^{E^*} + e_{31}^{*2}/\varepsilon_{33}^{S^*}} \tag{82}$$

and

$$\hat{K} = e_{31}^* h. \tag{83}$$

Note that $\bar{\hat{D}}$ and $\bar{\hat{\nu}}$ defined in Eq. (82) represents the effective flexural rigidity and the effective Poisson's ratio for the piezoceramic bimorph plate, respectively, and gives the same values as those obtained by Rogacheva (1994) with a different pair of constitutive equations and by Seok et al. (in press) with a different type of expansions of electric potentials. The same results can be obtained by expanding the electric potential with simple powers along the thickness co-ordinate, in which all the components of electric potential do not vary throughout the plane.

Introducing the strain–displacement relations into Eq. (81), the moments and the shear force resultants can be obtained in the form

$$\tau_a^{(1)} = \hat{K}V_e - \bar{\hat{D}}(w_{,a(a)} + \bar{\hat{\nu}}w_{,\bar{a}(\bar{a})}), \tag{84}$$

$$\tau_{3a}^{(0)} + \tau_{12,\bar{a}}^{(1)} = -\bar{\hat{D}}\{w_{,a(a)(a)} + (2\hat{r} - \bar{\hat{\nu}})w_{,a(\bar{a})(\bar{a})}\}, \tag{85}$$

where

$$\hat{r} = 2\tilde{D}/\bar{\hat{D}} + \bar{\hat{\nu}}. \tag{86}$$

Hence, the displacement equation of motion of the bimorph plate under the aforementioned conditions becomes

$$w_{,1111} + 2\hat{r}w_{,1122} + w_{,2222} + \bar{\hat{\kappa}}^2\ddot{w} = 0, \quad \bar{\hat{\kappa}} = \sqrt{2\rho h/\bar{\hat{D}}}. \tag{87}$$

Using Eqs. (84) and (85), the variational equation of the bimorph plate can be expressed in terms of the displacement along the x_3 direction and its derivatives.

The procedure to obtain the dispersion relations of this electrically simplified case is the same as that of the pure mechanical case. The differences exist only in the flexural rigidity and Poisson's ratio, which should be replaced with the effective ones defined in Eq. (82). For a low frequency range, the complex branches are not important because the imaginary number of the nearest complex branch to the origin is still large enough compared to the second imaginary branch, which is almost a straight line for the low frequency range. Although the L'Hospital theorem leads us to the limiting case solutions when the frequency approaches zero, the analytical derivation is rather cumbersome. However, using the binomial expansion, the limiting case for the imaginary branch can be calculated in a simple form for the symmetric modes. Note that only a part of the solutions symmetric with respect to the x_2 axis is of interest because only the symmetric modes are excited and suitable in the description of the bimorph plate employed in this work.

3.2. Reduction of the unelectroded bimorph plate equation

As a second case for the reduction, consider a unelectroded plate, which is thin enough to allow no variations along the x_3 axis. Since it is assumed that there is no charge just outside the body, the external electric intensity field is also treated to vanish. Therefore, it can be assumed that inside the plate for the thin piezoceramic plate, we have

$$D_3 = 0, \quad E_a = 0. \tag{88}$$

From the two-dimensional constitutive equations and the thin plate assumptions for electric quantities described in Eq. (88), the relation between the electric field intensity along the thickness direction and planar strains

$$E_3 = -e^*_{31}/\varepsilon^{S^*}_{33}\varepsilon_{aa} \tag{89}$$

can be obtained. Through the use of Eqs. (A.4) and (75), one may simply obtain the following equations:

$$\varepsilon^{S^*}_{33}\overset{(m)}{E}{}^{(n)}_3 + e^*_{31}\varepsilon^{(n)}_{aa} = 0; \quad \overset{(m)}{E}{}^{(n)}_3 = -\frac{e^*_{31}}{\varepsilon^{S^*}_{33}}\varepsilon^{(n)}_{aa}, \quad n = 0, 1. \tag{90}$$

With the aid of the assumption $\varepsilon^{(0)}_{aa} = 0$ for a thin bimorph plate, Eqs. (32), (34), (A.3) and (90) can give

$$w_{,1111} + 2\breve{r}\, w_{,1122} + w_{,2222} + \breve{\kappa}^2\ddot{w} = 0 \tag{91}$$

along with the two-dimensional constitutive equations

$$\tau^{(1)}_a = \breve{D}(\varepsilon^{(1)}_a + \breve{\nu}\,\varepsilon^{(1)}_{\bar{a}}) = -\breve{D}(w_{,a(a)} + \breve{\nu}\, w_{,\bar{a}(\bar{a})}), \tag{92}$$

$$\tau^{(0)}_{3a} + \tau^{(1)}_{12,\bar{a}} = -\breve{D}\{w_{,a(a)(a)} + (2\breve{r} - \breve{\nu})w_{,a(\bar{a})(\bar{a})}\}, \tag{93}$$

where

$$\breve{D} = \frac{2}{3}h^3\left(c^{E^*}_{11} + \frac{e^{*^2}_{31}}{\varepsilon^{S^*}_{33}}\right), \quad \breve{\nu} = \frac{(c^{E^*}_{11}\nu + e^{*^2}_{31}/\varepsilon^{S^*}_{33})}{(c^{E^*}_{11} + e^{*^2}_{31}/\varepsilon^{S^*}_{33})}, \quad \breve{r} = 2\tilde{D}/\breve{D} + \breve{\nu}, \quad \breve{\kappa} = \sqrt{2\rho h/\breve{D}}. \tag{94}$$

Note that $\breve{D}$ and $\breve{\nu}$ are the effective flexural rigidity and the effective Poisson's ratio for the unelectroded thin plate, respectively. The electric potential components can also be obtained successfully in the form

$$\overset{(m)}{E_3^{(0)}} = -\frac{1}{h}\left(\overset{(m)}{\varphi^{(1)}} + \hat{m}\,\overset{(m)}{\varphi^{(2)}}\right) = -\frac{e_{31}^*}{\varepsilon_{33}^{S^*}}\varepsilon_{aa}^{(0)} = 0, \tag{95}$$

$$\overset{(m)}{E_3^{(1)}} = -\frac{2}{h^2}\,\overset{(m)}{\varphi^{(2)}} = -\frac{e_{31}^*}{\varepsilon_{33}^{S^*}}\varepsilon_{aa}^{(1)} \tag{96}$$

along with the electric potential components in the form

$$\overset{(m)}{\varphi^{(n)}} = (-\hat{m})^n \frac{h^2}{2}\frac{e_{31}^*}{\varepsilon_{33}^{S^*}}\varepsilon_{aa}^{(1)}, \quad n = 1, 2. \tag{97}$$

4. Illustrative example: fully electroded and unelectroded bimorph plates made of PZT-5, *b*/*h* = 2

As an illustrative example of the resulting equations derived in the preceding sections, an infinitely long bimorph plate is considered. The plate is made of PZT-5 (Berlincourt et al., 1964) and have two facing edges free with width to height ratio $b/h = 2$. The mechanical and piezoelectrical properties of PZT-5 are shown in Table 1. Note that since the intrinsic modes of the rectangular bimorph plate induced by the electric field applied to the major surfaces are symmetric with respect to the x_1 axis, dispersion relations for anti-symmetric modes naturally vanish; only symmetric modes exist.

The dispersion relations for the bimorph plate with electrodes that entirely cover the major surfaces, with the quantity $3\hat{D}/2h^3 = 6.965 \times 10^{11}$ Pa and effective Poisson's ratio $\hat{\nu} = 0.351$, are obtained for the frequency and wave number ranges of interest here. The dispersion curves shown in Fig. 2 are drawn with the data obtained from the computer program using a symbolic programming language, Maple (1997). Computations have been made separately with quadruple precision to reduce possible errors originated from the large non-propagating wave numbers. In this figure, the dimensionless frequency $\bar{\Omega}$ is plotted against $\Re(\bar{\xi})$ and $\Im(\bar{\xi})$ over a range up to a unity near $\bar{\Omega} = 0$. Here, $\Re(\bar{\xi})$ and $\Im(\bar{\xi})$ represents the real and the imaginary part of the dimensionless wave number $\bar{\xi}$, respectively. It may be informative if real dimensions are taken for the calculation to give physical insights. For the bimorph plate with thickness $h = 10\,\mu$m as an example, the upper limit of the figure $\bar{\Omega} = 1$ corresponds to $\omega = 1.34 \times 10^8$ rad/s, or equiv-

Table 1
Three-dimensional piezoelectric constants of PZT-5 (taken from Berlincourt et al., 1964)

Property	PZT-5	Unit
c_{11}^E	12.1×10^{10}	Pa
c_{12}^E	7.54×10^{10}	Pa
c_{13}^E	7.52×10^{10}	Pa
c_{33}^E	11.1×10^{10}	Pa
c_{44}^E	2.11×10^{10}	Pa
c_{66}	2.26×10^{10}	Pa
e_{31}	-5.4	C/m^2
e_{33}	15.8	C/m^2
e_{15}	12.3	C/m^2
$\varepsilon_{11}^S/\varepsilon_0$	916	–
$\varepsilon_{33}^S/\varepsilon_0$	830	–
ε_0	8.85×10^{-12}	F/m
ρ	7.75×10^3	kg/m^3

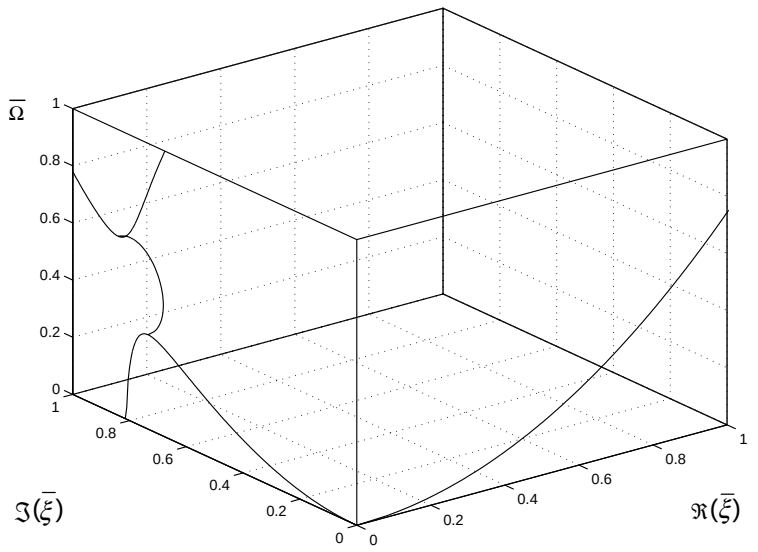

Fig. 2. Dispersion relations for symmetric modes of a fully electroded bimorph plate.

alently, 21.3 MHz, which is sufficiently high for the flexural vibrations of bimorph plates under consideration. As can be expected, the complex wave numbers appear in pairs, which are known to be associated with edge vibrations in bounded plate (Mindlin, 1960). Observing the shapes of the dispersion curves, they are quite similar to those of purely mechanical case (Seok et al., 2004). There are two branches dominating the dynamics of the plate for the plates having large length to width ratio; one is real and the other is imaginary close to the origin. The second imaginary branch needs also to be included, especially for the plate that has free corners thus requires to satisfy Kirchhoff corner conditions, in order to satisfy boundary conditions given to other edges as much as possible. Special attention needs to be taken for the complex wave branches since the complex conjugate must also be included. In that case, the magnitudes associated with a complex pair are not independent; hence their variations are not. However, the real and the imaginary part of the wave number can vary freely.

The dispersion relations for the bimorph plate without electrodes on the major surfaces are also obtained and depicted in Fig. 3. For the low frequency range ($\bar{\Omega} \ll 1$), the dispersion curves are similar to those of the fully electroded case. However, the second imaginary branch locates higher than that of the fully electroded case.

The dispersion curves for the fully electroded bimorph plate using the reduced equation (82) developed in Section 3.1 are shown in Fig. 4, in which effective Poisson's ratio $\bar{\tilde{\nu}} = 0.408$ and normalized flexural rigidity $\bar{\tilde{D}}/\hat{D} = 1.097$ are obtained for PZT-5. Comparing the dispersion curves with those of the fully electroded bimorph plate within a low frequency range, the deviations between the two branches of a kind are pretty small. Hence, to reduce the matrix size, this reduced equation with the effective flexural rigidity and Poisson's ratio can be employed for the approximations in a low frequency range.

The dispersion curves, with effective Poisson's ratio $\breve{\nu} = 0.532$ and normalized flexural rigidity $\breve{D}/\hat{D} = 1.388$, can be drawn by inserting the solution functions obtained from the governing differential equation, Eq. (91), which are shown in Fig. 5 based on Eqs. (92) and (93).

Comparing the dispersion curves depicted in Fig. 5 to that with the non-reduced differential equations (Fig. 3) it can be found that the two figures are almost identical. Hence, even in the higher range of the frequency, the results with the reduced equation would be very close to those with fully coupled

equations, which could validate the usage of the reduced equations for a relatively wider frequency range.

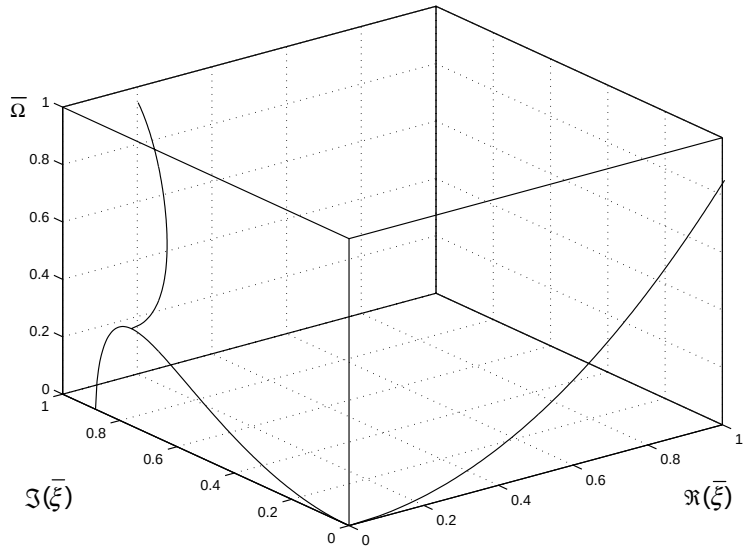

Fig. 3. Dispersion relations for symmetric modes of a unelectroded bimorph plate.

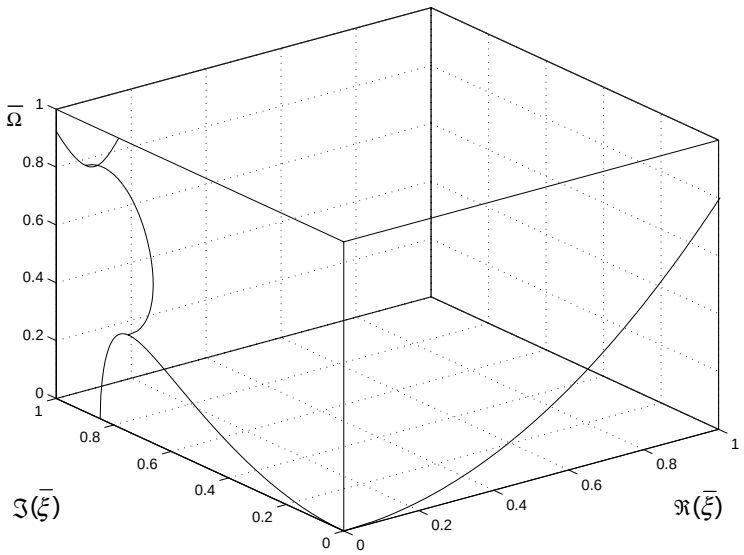

Fig. 4. Dispersion curves for symmetric modes of a fully electroded bimorph plate with the reduction of equations.

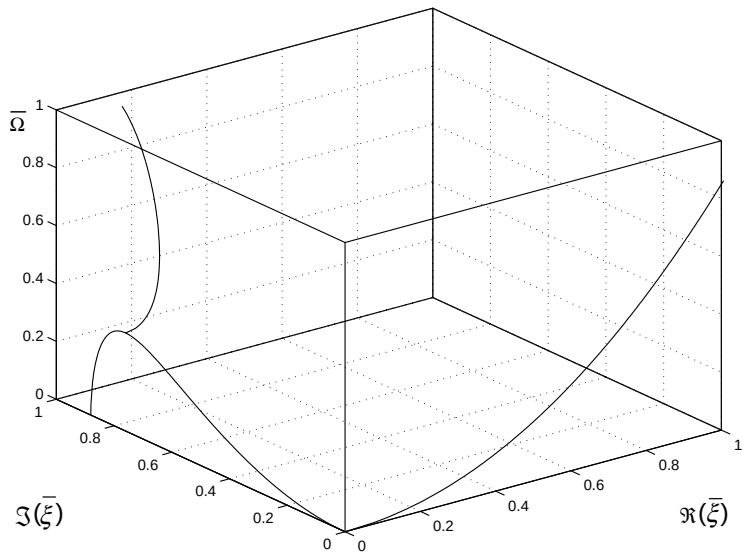

Fig. 5. Dispersion curves for symmetric modes of a unelectroded bimorph plate with the reduction of equations.

5. Conclusions

A procedure to obtain the dispersion relations of bimorph plates with two facing edges free for fully electroded and unelectroded major surfaces has been proposed. Coupled differential equations as well as dispersion relations subject to homogeneous constraint-type boundary conditions on the two facing side-edges have been derived for both fully electroded and unelectroded bimorph plates through the expansions of electric potential in the thickness co-ordinate with vanishing second order components of electric potentials at major surfaces in the manner of Tiersten. Successive reduction procedures for both fully electroded and unelectroded cases have also been developed.

Dispersion curves for the aforementioned four cases have been depicted for the bimorph plate of PZT-5 with a fixed width to height ratio $b/h = 2$. Comparisons have been made and have shown that the reductions can be successfully employed in the variational approximation procedure in a good accuracy for a relatively wider frequency range.

Appendix A. Series expansions of mechanical stress and electric displacement resultants

For the purpose of obtaining the two-dimensional constitutive equations of the thin bilayered bimorph plate, integrating Eq. (5) over the thickness of each layer after multiplying x_3^n, with plane stress assumptions, we obtain

$$\overset{(m)}{\tau}{}_a^{(n)} = \hat{m} \sum_{k=0}^{1} \left\{ c_{11}^{E^*} \frac{(-\hat{m}h)^{n+k+1}}{(n+k+1)} (\varepsilon_a^{(k)} + \nu \varepsilon_{\bar{a}}^{(k)}) - e_{31}^{*} \frac{(-\hat{m}h)^{n+k+1}}{(n+k+1)} \overset{(m)}{E}{}_3^{(k)} \right\}, \tag{A.1}$$

where $m = 1, 2$, $n = 0, 1$, and the continuity conditions of ε_{ab} across the middle plane have already been taken into consideration. In Eq. (A.1) we have also introduced the series expansion of elastic strain along the thickness co-ordinate (Seok et al., 2004)

$$\varepsilon_{ab} = \sum_{n=0}^{1} \varepsilon_{ab}^{(n)} x_3^n. \tag{A.2}$$

Note that the stress continuity conditions are satisfied trivially due to the plane stress assumptions of $\tau_{3j} = 0$. Furthermore, due to the plane stress assumptions for free thickness strains, the stress components in x_3 direction may be ignored.

For the future usage, it is profitable to write the normal stress resultants for the first order: [3]

$$\overset{(m)}{\tau}{}_a^{(1)} = -c_{11}^{E^*}\left\{\hat{m}\frac{h^2}{2}\left(\varepsilon_a^{(0)} + v\varepsilon_{\bar{a}}^{(0)}\right) - \frac{h^3}{3}\left(\varepsilon_a^{(1)} + v\varepsilon_{\bar{a}}^{(1)}\right)\right\} + e_{31}^*\left(\hat{m}\frac{h^2}{2}\overset{(m)}{E}{}_3^{(0)} - \frac{h^3}{3}\overset{(m)}{E}{}_3^{(1)}\right). \tag{A.3}$$

The nth order components of electric displacement in the x_3 direction can be calculated, from Eq. (12) with the aid of Eq. (3) along with the plane stress assumptions, in the form

$$\begin{aligned}
\overset{(1)}{D}{}_3^{(n)} &= \int_{0^+}^{h} \overset{(1)}{D}_3 x_3^n \,\mathrm{d}x_3 \\
&= \varepsilon_{33}^{S^*}\left\{\frac{h^{n+1}}{(n+1)}\overset{(1)}{E}{}_3^{(0)} + \frac{h^{n+2}}{(n+2)}\overset{(1)}{E}{}_3^{(1)}\right\} + e_{31}^*\left\{\frac{h^{n+1}}{(n+1)}(\varepsilon_1^{(0)} + \varepsilon_2^{(0)}) + \frac{h^{n+2}}{(n+2)}(\varepsilon_1^{(1)} + \varepsilon_2^{(1)})\right\}, \\
\overset{(2)}{D}{}_3^{(n)} &= \int_{-h}^{0^-} \overset{(2)}{D}_3 x_3^n \,\mathrm{d}x_3 \\
&= -\varepsilon_{33}^{S^*}\left\{\frac{(-h)^{n+1}}{(n+1)}\overset{(2)}{E}{}_3^{(0)} + \frac{(-h)^{n+2}}{(n+2)}\overset{(2)}{E}{}_3^{(0)}\right\} - e_{31}^*\left\{\frac{(-h)^{n+1}}{(n+1)}(\varepsilon_1^{(0)} + \varepsilon_2^{(0)}) + \frac{(-h)^{n+2}}{(n+2)}(\varepsilon_1^{(1)} + \varepsilon_2^{(1)})\right\},
\end{aligned} \tag{A.4}$$

where the two-dimensional electric permittivity

$$\varepsilon_{33}^{S^*} = \varepsilon_{33}^S + e_{33}^2/c_{33}^E \tag{A.5}$$

has been newly introduced. Since all the shear stresses on the major surfaces of the plate have been neglected on account of the plane stress assumptions, the substitution of Eqs. $(3)_4$ and $(3)_5$ into Eqs. $(3)_7$ and $(3)_8$ yields

$$D_a = \varepsilon_{11}^{S^*} E_a, \quad a = 1, 2, \tag{A.6}$$

where

$$\varepsilon_{11}^{S^*} = \varepsilon_{11}^S - e_{15}^2/c_{44}^E. \tag{A.7}$$

Multiplying Eq. (A.6) by x_3^n and integrating the resulting equation over the thickness of each layer, the nth order components of electric displacement in the planar directions can be obtained in the form

$$\overset{(m)}{D}{}_a^{(n)} = -\hat{m}\varepsilon_{11}^{S^*}\sum_{k=0}^{2}\frac{(-\hat{m}h)^{n+k+1}}{n+k+1}\overset{(m)}{E}{}_a^{(k)}, \quad m = 1, 2, \quad n = 0, \ldots, 2, \tag{A.8}$$

where

[3] Since the bimorph plate produces the flexural motion only, the variational equation for the out-of-plane motion is necessary and sufficient in this description.

$$\overset{(m)}{E}{}_a^{(0)} = 0, \quad \overset{(m)}{E}{}_a^{(1)} = -\frac{\hat{m}}{h}\overset{(m)}{\varphi}{}_{,a}^{(2)}, \quad \overset{(m)}{E}{}_a^{(2)} = -\frac{1}{h^2}\overset{(m)}{\varphi}{}_{,a}^{(2)}, \ m = 1, 2. \tag{A.9}$$

Appendix B. Relations between electric current and displacement gradient for a fully electroded bimorph plate subject to a prescribed surface charge

Consider a bimorph plate with a measurement set-up as depicted in Fig. 6. Although two different gauges may be used for the two different layers in this configuration, both readings would indicate the same absolute values due to the symmetry of the geometry and material properties.

The electric part of the variational equation of the fully electroded bimorph plate used for the purpose of sensing the vibrations may take the form

$$\begin{aligned}\int_{t_0}^{t} \mathrm{d}t \sum_{m=1}^{2} \Bigg[\int_{\hat{S}} \Bigg\{ \left(\overset{(m)}{D}{}_{a,a}^{(0)} + \overset{(m)}{d}{}_3^{(0)} \right) \delta \overset{(m)}{\varphi}{}^{(0)} + \frac{1}{h} \left(\overset{(m)}{D}{}_{a,a}^{(1)} - \overset{(m)}{D}{}_3^{(0)} + \overset{(m)}{d}{}_3^{(1)} \right) \delta \overset{(m)}{\varphi}{}^{(1)} \\ + \frac{1}{h^2} \left(\overset{(m)}{D}{}_{a,a}^{(2)} + \hat{m}h \overset{(m)}{D}{}_{a,a}^{(1)} - 2\overset{(m)}{D}{}_3^{(1)} - \hat{m}h \overset{(m)}{D}{}_3^{(0)} \right) \delta \overset{(m)}{\varphi}{}^{(2)} \Bigg\} \mathrm{d}S - \int_{\hat{S}} \Big[\{ [\bar{\sigma} + D_3]_{x_3=h} + [\bar{\sigma} - D_3]_{x_3=0^+} \} \delta \overset{(1)}{\varphi}{}^{(0)} \\ + \{ [\bar{\sigma} - D_3]_{x_3=-h} + [\bar{\sigma} + D_3]_{x_3=0^-} \} \delta \overset{(2)}{\varphi}{}^{(0)} \Big] \mathrm{d}S - \int_{\hat{S}} \Big\{ [\bar{\sigma} + D_3]_{x_3=h} \delta \overset{(1)}{\varphi}{}^{(1)} + [\bar{\sigma} - D_3]_{x_3=-h} \delta \overset{(2)}{\varphi}{}^{(1)} \Big\} \mathrm{d}S \Bigg], \end{aligned} \tag{B.1}$$

where

$$\overset{(1)}{d}{}_3^{(0)} = [D_3]_{0^+}^{h}, \quad \overset{(2)}{d}{}_3^{(0)} = [D_3]_{-h}^{0^-}. \tag{B.2}$$

Keeping in mind the fact that the first order components of the electric potential do not vary with position, the differential and the integral equations can be obtained from the variational equation in the form

$$\oint_{\overset{(m)}{C}} n_a \overset{(m)}{D}{}_a^{(0)} \, \mathrm{d}s + \int_{\hat{S}} \overset{(m)}{d}{}_3^{(0)} \, \mathrm{d}S = 0, \tag{B.3}$$

$$\oint_{\overset{(m)}{C}} n_a \overset{(m)}{D}{}_a^{(1)} \, \mathrm{d}s - \int_{\hat{S}} \overset{(m)}{D}{}_3^{(0)} \, \mathrm{d}S + \int_{\hat{S}} \overset{(m)}{d}{}_3^{(1)} \, \mathrm{d}S = 0, \tag{B.4}$$

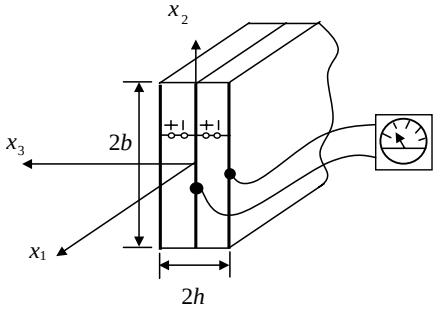

Fig. 6. Schematic view of a sensing bimorph plate with its co-ordinate system.

$$\overset{(m)}{D}{}^{(2)}_{a,a} + \hat{m}h\overset{(m)}{D}{}^{(1)}_{a,a} - 2\overset{(m)}{D}{}^{(1)}_{3} - \hat{m}h\overset{(m)}{D}{}^{(0)}_{3} = 0. \tag{B.5}$$

Similarly, the boundary part of Eq. (B.1) gives the following integral form of boundary conditions:

$$\int_{\hat{S}} \{D_3(h) - D_3(0^+)\}\,\mathrm{d}S = \int_{\hat{S}} -\{\bar{\sigma}(h) + \bar{\sigma}(0^+)\}\,\mathrm{d}S, \tag{B.6}$$

$$\int_{\hat{S}} \{-D_3(-h) + D_3(0^-)\}\,\mathrm{d}S = \int_{\hat{S}} -\{\bar{\sigma}(-h) + \bar{\sigma}(0^-)\}\,\mathrm{d}S, \tag{B.7}$$

$$\int_{\hat{S}} D_3(h)\,\mathrm{d}S = -\int_{\hat{S}} \bar{\sigma}(h)\,\mathrm{d}S, \tag{B.8}$$

$$\int_{\hat{S}} D_3(-h)\,\mathrm{d}S = \int_{\hat{S}} \bar{\sigma}(-h)\,\mathrm{d}S, \tag{B.9}$$

where the symbols in the parenthesis represent the position on the x_3 axis.

Referring to Eq. (A.8), the electric displacement components can be expressed as functions of electric potential components in the form

$$\overset{(m)}{D}{}^{(0)}_{a} = \frac{h}{6}\varepsilon^{S^*}_{11}\overset{(m)}{\varphi}{}^{(2)}_{,a}, \quad \overset{(m)}{D}{}^{(1)}_{a} = -\hat{m}\frac{h^2}{3}\varepsilon^{S^*}_{11}\overset{(m)}{\varphi}{}^{(2)}_{,a}, \quad \overset{(m)}{D}{}^{(2)}_{a} = \frac{h^3}{20}\varepsilon^{S^*}_{11}\overset{(m)}{\varphi}{}^{(2)}_{,a}. \tag{B.10}$$

Hence, the two differential equations obtained from the mechanical and electrical parts of the variational equation can be given by the same form as those obtained under the prescribed voltage, Eqs. (35) and (39), since the first order component of the electric potential for each layer is independent of the position.

From the first integral equation, Eq. (B.3), the relations of the x_3 directional electric displacement components between the two electrodes can be obtained if $\overset{(m)}{D}{}^{(0)}_{a}$ are given from the electric continuity condition $n_a \underset{\sim}{[}\, \overset{(2)}{D}{}^{(0)}_{a} \,\underset{\sim}{]} = 0$ with the convention $\underset{\sim}{[}\, a \,\underset{\sim}{]} = a^+ - a^-$. For the case when the dielectric constant in the material just outside the bimorph plate is much larger than that in the bimorph plate, one may have the relations

$$\int_{\hat{S}} D_3(h)\,\mathrm{d}S = \int_{\hat{S}} D_3(0^+)\,\mathrm{d}S = -\int_{\hat{S}} \bar{\sigma}(h)\,\mathrm{d}S = \int_{\hat{S}} \bar{\sigma}(0^+)\,\mathrm{d}S, \tag{B.11}$$

$$\int_{\hat{S}} D_3(-h)\,\mathrm{d}S = \int_{\hat{S}} D_3(0^-)\,\mathrm{d}S = \int_{\hat{S}} \bar{\sigma}(-h)\,\mathrm{d}S = -\int_{\hat{S}} \bar{\sigma}(0^-)\,\mathrm{d}S. \tag{B.12}$$

If the total amount of prescribed surface charge on the middle electrode is denoted as $2\bar{q}$, Eqs. (B.11) and (B.12) give the following relations:

$$\int_{\hat{S}} \bar{\sigma}(0^+)\,\mathrm{d}S = \int_{\hat{S}} \bar{\sigma}(0^-)\,\mathrm{d}S = +\bar{q}, \tag{B.13}$$

$$\int_{\hat{S}} \bar{\sigma}(h)\,\mathrm{d}S = \int_{\hat{S}} \bar{\sigma}(-h)\,\mathrm{d}S = -\bar{q}. \tag{B.14}$$

Finally Eqs. (B.11)–(B.14) give the third term in integral equation (B.4) with the result

$$\int_{S} \overset{(m)}{d}{}^{(1)}_{3}\,\mathrm{d}S = -\hat{m}h\bar{q}. \tag{B.15}$$

Through the use of Eq. (A.4), the first term in integral equation (B.4) can be transformed into more convenient form with the components of the electrical potential and the strain, which has the same form as Eq. (54)

$$\overset{(m)}{D}{}_3^{(0)} = -\varepsilon_{33}^{S^*}\overset{(m)}{\varphi}{}^{(1)} - \hat{m}e_{31}^* h^2 \varepsilon_{aa}^{(1)}/2. \tag{B.16}$$

The insertion of Eq. (B.16) in integral equation (B.4), and then the introduction of the strain–displacement relations finally yields the relations between the electrical potential, displacement, and the prescribed total surface charge with the result

$$\varepsilon_{33}^{S^*}\int_S \overset{(m)}{\varphi}{}^{(1)}\,\mathrm{d}S - \hat{m}\left(\frac{e_{31}^* h^2}{2}\int_S w_{,aa}\,\mathrm{d}S + h\bar{q}\right) = 0. \tag{B.17}$$

The rearrangement of Eq. (B.17) for $\overset{(m)}{\varphi}{}^{(1)}$ yields

$$\overset{(m)}{\varphi}{}^{(1)} = \frac{\hat{m}}{\varepsilon_{33}^{S^*}S}\left(h\bar{q} + \frac{e_{31}^* h^2}{2}\int_S w_{,aa}\,\mathrm{d}S\right). \tag{B.18}$$

These equations state that the resulting voltage or charge induced by the deformation of the plate can be obtained with given electrical and geometrical quantities when either charge or voltage is prescribed, or the relation between the two is known. The rearrangement of Eq. (B.18), after the differentiation with time, yields the current equation in the form

$$\overset{(m)}{I} = \dot{\bar{q}} = \frac{\mathrm{i}\omega}{\hat{m}h}\left(\varepsilon_{33}^{S^*}S\,\overset{(m)}{\varphi}{}^{(1)} - \hat{m}\frac{e_{31}^* h^2}{2}\int_S w_{,aa}\,\mathrm{d}S\right), \tag{B.19}$$

which effectively shows the same result given by Keuning (1971).

Eq. (B.19) still requires a relation between the current and the electrical potential since these quantities are not independent once an external-measuring circuit is connected. If the electrodes are connected by a contour with known complex conductivity

$$\overset{(m)}{Y} = \overset{(m)}{Y}_{\mathrm{R}} + \mathrm{i}\,\overset{(m)}{Y}_{\mathrm{I}}, \tag{B.20}$$

then the induced current can be connected with electrical potential via

$$\overset{(m)}{I} = \overset{(m)}{Y}\left[\overset{(m)}{\varphi}\right]_{x_3=-\hat{m}h}. \tag{B.21}$$

The substitution of Eq. (B.21) for $\overset{(m)}{\varphi}$ into Eq. (B.19) yields

$$\overset{(m)}{I} = -\frac{\mathrm{i}\omega}{h}\frac{e_{31}^* h^2}{2}\int_S w_{,aa}\,\mathrm{d}S \Bigg/ \left(1 - \frac{\mathrm{i}\omega\varepsilon_{33}^{S^*}S}{\hat{m}\,\overset{(m)}{Y}\,h}\right). \tag{B.22}$$

This completes the relation between the induced current and the deformation due to the motion of the plate. For a special case of $|\mathrm{i}\omega\varepsilon_{33}^{S^*}S/(\overset{(m)}{Y}\,h)| \ll 1$, Eq. (B.22) gives a simplified current-deformation relation in the form

$$\overset{(m)}{I} = -\frac{\mathrm{i}\omega}{h}\frac{e_{31}^* h^2}{2}\int_S w_{,aa}\,\mathrm{d}S. \tag{B.23}$$

Similarly, if the voltage is prescribed, Eq. (B.19) can be used for the calculation of the current induced by the deflection with the opposite sign to the previous case following the electrical convention of Skilling (1959). [4] From the integral equation (B.4), the current in the bimorph plate subject to a prescribed voltage can be calculated as

$$\overset{(m)}{I} = \overset{(m)}{I_V} + \overset{(m)}{I_D}, \tag{B.24}$$

where

$$\overset{(m)}{I_V} = -\frac{\mathrm{i}\omega}{h}\varepsilon_{33}^{S^*} S V_{\mathrm{e}}, \quad \overset{(m)}{I_D} = -\frac{\mathrm{i}\omega}{h}\frac{e_{31}^{*} h^2}{2}\int_S w_{,aa}\,\mathrm{d}S. \tag{B.25}$$

Note that $\overset{(m)}{I_V}$ means the current due to applied voltage source and $\overset{(m)}{I_D}$ represents the current induced by the deflection of the mth layer of the plate.

References

Anderson, E.H., Hagood, N.W., 1990. Simultaneous piezoelectric sensing/actuator: analysis and application to controlled structures. Journal of Sound and Vibration 174, 617–639.

Berlincourt, D.A., Curran, D.R., Jaffe, H., 1964. Piezoelectric and piezomagnetic materials and their function as transducers. In: Mason, W.P. (Ed.), Physical Acoustics, vol. 1 Part A. Academic Press, New York.

Chen, C., Wang, X., Shen, Y., 1996. Finite element approach of vibration control using self-sensing piezoelectric actuators. Computers & Structures 60, 505–512.

Cheng, Z.-Q, Lim, C.W., Kitipornchai, S., 1999. Three-dimensional exact solution for inhomogeneous and laminated piezoelectric plates. International Journal of Engineering Sciences 37, 1425–1439.

Cheng, Z.-Q, Lim, C.W., Kitipornchai, S., 2000. Three-dimensional asymptotic approach to inhomogeneous and laminated piezoelectric plates. International Journal of Solids and Structures 37, 3153–3175.

Fernandes, A., Pouget, J., 2003. Analytical and numerical approaches to piezoelectric bimorph. International Journal of Solids and Structures 40, 4331–4352.

He, L.H., Lim, C.W., Soh, A.K., 2000. Three-dimensional analysis of an antiparallel piezoelectric bimorph. Acta Mechanica 145, 189–204.

IEEE std. 176, 1978. IEEE Standard on Piezoelectricity. Institute of Electrical and Electronics Engineers, New York.

Keuning, D.H., 1971. Approximate equations for the flexure of thin, incomplete, piezoelectric bimorphs. Journal of Engineering Mathematics 5, 307–319.

Lanczos, C., 1949. The Variational Principles of Mechanics. University of Toronto Press, Toronto.

Lee, P.C.Y., Syngellakis, S., Hou, J.P., 1987. A two-dimensional theory for high-frequency vibrations of piezoelectric crystal plates with or without electrodes. Journal of Applied Physics 61, 1249–1262.

Lim, C.W., He, L.H., 2001. Exact solution of a compositionally graded piezoelectric layer under uniform stretch, bending and twisting. International Journal of Mechanical Sciences 43, 2479–2492.

Lim, C.W., He, L.H., Soh, A.K., 2001. Three-dimensional electromechanical responses of a parallel piezoelectric bimorph. International Journal of Solids and Structures 38, 2833–2849.

Low, T.S., Guo, W., 1995. Modeling of a three-layer piezoelectric bimorph beam with hysteresis. Journal of Microelectromechanical Systems 4, 230–237.

Maple™ V Release 5, 1997. Waterloo Maple Inc.

Mason, W.P., 1964Physical Acoustics, vol. 1 Part A. Academic Press, New York and London.

Mindlin, R.D., 1955. An Introduction to the Mathematical Theory of the Vibration of Elastic Plates. US Army Signal Corps Engineering Laboratory, Fort Monmouth, New Jersey.

Mindlin, R.D., 1960. Structural Mechanics 199-232. In: Goodier, J.N., Hoff, N.J. (Eds.), Waves and Vibrations in Isotropic Elastic Plates. Pergamon Press, Oxford, London.

Rao, S.S., Sunar, M., 1994. Piezoelectricity and its use in disturbance sensing and control of flexible structures: a survey. ASME Applied Mechanics Reviews 47, 113–123.

[4] Electric current is considered positive if it flows from active to passive + to +.

Ricketts, D., 1993. Transverse vibrations of composite piezoelectric polymer plates. Journal of Acoustical Society of America 77, 1939–1945.

Rogacheva, N.N., 1994. The Theory of Piezoelectric Shells and Plates. CRC Press, London.

Rogacheva, N.N., Chou, C.C., Chang, H., 1998. Electromechanical analysis of a symmetric piezoelectric/elastic laminate structure: theory and experiment. IEEE Transactions on Ultrasonics, Ferroelectrics, and Frequency Control 45, 285–294.

Seok, J., 2001. Vibratory angular rate gyroscope using polarized piezoceramic bimorphs. Ph.D. Dissertation, Rensselaer Polytechnic Institute.

Seok, J., Tiersten, H.F., Scarton, H.A., 2004. Free vibrations of rectangular cantilever plates. Part 1: out-of-plane motion. Journal of Sound and Vibration 271, 131–146.

Seok, J., Tiersten, H.F., Scarton, H.A., in press. An analysis of a vibratory angular-rate gyroscope using polarized piezoceramic bimorph plates. Part 1: derivation of variational equations in the absence of angular velocity. Journal of Sound and Vibration.

Skilling, H.H., 1959. Electrical Engineering Circuits. John Wiley & Sons Inc., New York.

Smits, J.G., Choi, W., 1991. The constituent equations of piezoelectric heterogeneous bimorphs. IEEE Transactions on Ultrasonics, Ferroelectrics, and Frequency Control 38, 256–270.

Steel, M.R., Harrison, F., Harper, P.G., 1978. The piezoelectric bimorph: an experimental and theoretical study of its quasistatic response. Journal of Physics D: Applied Physics 11, 979–989.

Stewart, J.T., Yong, Y.-K., 1994. Exact analysis of the propagation of acoustic waves in multilayered anisotropic piezoelectric plates. IEEE Transactions on Ultrasonics, Ferroelectrics, and Frequency Control 41, 375–390.

Tiersten, H.F., 1969. Linear Piezoelectric Plate Vibrations. Plenum Press, New York.

Tiersten, H.F., 1993. Electroelastic equations for electroded thin plates subject to large driving voltages. Journal of Applied Physics 73, 3389–3393.

Tiersten, H.F., 1995. Equations for the control of the flexural vibrations of composite plates by partially electroded piezoelectric actuators. Active Materials and Smart Structures, SPIE 2427, 326–342.

Yong, Y.-K., Stewart, J.T., Ballato, A., 1993. A laminated plate theory for high frequency, piezoelectric thin-film resonators. Journal of Applied Physics 74, 3028–3046.